

Spontaneous synchronization and quantum correlation dynamics of open spin systemsG. L. Giorgi,^{1,2} F. Plastina,^{3,4} G. Francica,³ and R. Zambrini⁵¹*INRIM, Strada delle Cacce 91, I-10135 Torino, Italy*²*AG Theoretische Quantenphysik, Theoretische Physik, Universität des Saarlandes, D-66123 Saarbrücken, Germany*³*Dipartimento di Fisica, Università della Calabria, 87036 Arcavacata di Rende (CS), Italy*⁴*INFN-Gruppo collegato di Cosenza, Cosenza, Italy*⁵*IFISC (UIB-CSIC), Instituto de Física Interdisciplinar y Sistemas Complejos, UIB Campus, E-07122 Palma de Mallorca, Spain*

(Received 8 May 2013; published 21 October 2013)

We discuss the emergence of spontaneous synchronization for an open spin-pair system interacting only via a common environment. Under suitable conditions, and even in the presence of detuning between the natural precession frequencies of the two spins, they are shown to reach a long-lasting transient behavior where they oscillate in phase. We explore the connection between the emergence of such a behavior and the establishment of robust quantum correlations between the two spins, analyzing differences between dissipative and dephasing effects. In particular, in the regime in which synchronization occurs, quantum correlations are more robust for shorter synchronization times and this is related to a separation between system decay rates.

DOI: [10.1103/PhysRevA.88.042115](https://doi.org/10.1103/PhysRevA.88.042115)

PACS number(s): 03.65.Yz, 05.45.Xt, 75.10.Dg

I. INTRODUCTION

Synchronization is a paradigmatic phenomenon in complex systems, characterized by a coherent dynamics of different oscillating units [1,2]. Spontaneous synchronization generally arises in spite of detuning of the natural frequencies of component subsystems, due to their weak interaction. After more than three centuries from the first reported observation [3], this phenomenon has been identified in several physical, biological, chemical, and social systems [1,2,4]. At the microscopic level, mutual synchronization has been studied in different devices, such as arrays of Josephson junctions [5], spin torque nano-oscillators [6], and nanomechanical [7] and optomechanical oscillators [8–11]. Most of these implementations at micro- and nanoscale have focused on the classical dynamics, while quantum fluctuations and correlations have been analyzed in [11–14].

A full quantum approach has been recently reported for forced synchronization by Goychuk *et al.* [15] considering quantum stochastic synchronization in the spin-boson dynamics in the presence of a driving signal modulated in time and reporting on the constructive role of thermal noise. Furthermore, synchronization with driving was considered by Zhirov and Shepelyansky, who discussed the effect of a driven resonator in the cases of both one [16] and two superconducting qubits [17]. These works explore the phenomena of forced synchronization, usually referred to as entrainment, in the quantum regime where the system synchronizes with the external driver instead of following its natural frequency. The presence of driving out of equilibrium does also favor quantum effects [18].

On the other hand, *spontaneous* or mutual synchronization between detuned coupled systems is the coherent dynamic phenomenon of rhythm adjustment without any external driver taming the evolution. The emergence of spontaneous quantum synchronization has been recently considered for dissipative harmonic oscillators with two major breakthroughs: (i) the possibility to have synchronization induced by dissipation in a linear system and (ii) the full quantumness of this phenomenon (reported for vacuum fluctuations) [12–14]. Synchronous

dynamics has been reported during the relaxation process, in spite of the diversity of the natural frequencies of a pair of oscillators [12], due to the occurrence of a slowly decaying mode responsible for synchronization accompanied by robust and asymptotic quantum correlations in the system [12,13]. Interestingly, if the oscillators experience losses in separate baths, synchronization does not emerge, independently of the strength of their coupling [12]. When more than two detuned oscillators are considered and depending on the environment correlation length, synchronization and robust quantum correlations can arise not only in a transient but even *asymptotically* [13,14], associated with the presence of some decoherence-free normal mode of the system, as reported even for random networks [14].

A main open question is about the possibility to induce synchronization in the presence of a different kind of coupling to the environment, giving rise to dephasing rather than dissipation. In this paper, we tackle this question by discussing the dynamics of two precessing spins [see Fig. 1] detuned from each other and experiencing decoherence due to the coupling with an environment, with the aim of assessing in such a framework the key mechanism responsible for quantum synchronization. As for the case of quantum oscillators [14], we will show that the form of the coupling with the bath is a crucial ingredient for a synchronous dynamics to emerge between detuned quantum subsystems relaxing towards equilibrium. In order to establish their distinctive roles, both a dissipative and a purely dephasing spin dynamics will be studied, and, through a sensible parametrization of the system-bath interaction, a continuous transition between these two extreme cases will be considered.

Another question that naturally arises about synchronization in the quantum regime is whether it is related to the appearance of entanglement or of more general quantum correlations, measured, e.g., by quantum discord whose dynamics has been studied extensively for a detuned spin pair in a common environment (see, for instance, Refs. [19,20]).

Comparing with previous works on synchronization in the quantum regime [8–14,21], an important difference is that we are going to consider spins that are not directly coupled to each

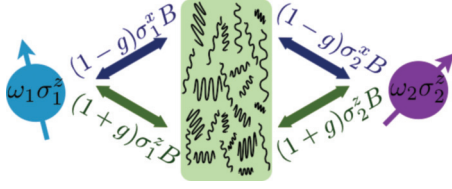


FIG. 1. (Color online) Schematics of the system. Two spins interact with a common thermal bosonic environment [and specifically to the quantum and thermal fluctuations of the environmental operator $B = \sum_k \gamma_k (a_k^\dagger + a_k)$] through the two different coupling mechanisms reported in Eq. (3). The first coupling term, $\alpha(1+g)\sigma_i^z$, only induces pure dephasing, while the second one, $\alpha(1-g)\sigma_i^x$ ($i = 1, 2$), is also a source of dissipation.

other, so that spontaneous synchronization as well as quantum correlations only arise due to the indirect, bath-mediated coupling. Mutual synchronization in nonresonant spin systems was also studied by Orth *et al.* in Ref. [22], analyzing the case of two spins coupled to each other via an Ising-like term and strongly interacting with a common bath, which induces a substantial renormalization of the coupling strength. Under these conditions, a few correlated and synchronous oscillations are observed before dissipation prevails. Here, instead, we are going to consider the weak-coupling regime between spins and bath, to show that a long-time, robust, synchronous dynamics occurs, even in the absence of a direct coupling between the subsystems.

II. DESCRIPTION OF THE MODEL

We consider two noninteracting qubits with different precession frequencies ω'_1 and ω'_2 and coupled to a common thermal bath. By employing units in which $\hbar = 1$, the system Hamiltonian can be written as

$$H_S = \omega_1 \sigma_1^z + \omega_2 \sigma_2^z, \quad (1)$$

where $\omega_1 = \omega'_1/2$ and $\omega_2 = \omega'_2/2$. The common thermal environment is modeled as a set of independent harmonic oscillators, $H_B = \sum_k \Omega_k a_k^\dagger a_k$, taken in its thermal state $\rho_B = \exp[-\beta H_B]/\text{Tr}\{\exp[-\beta H_B]\}$, and the system-bath interaction term has the form

$$H_{SB} = V_S \sum_k \gamma_k (a_k^\dagger + a_k). \quad (2)$$

A sketch of the model is given in Fig. 1. Generically, in a spin-boson problem, the environmental fluctuations are coupled both longitudinally and transversally to the spin, e.g., via interaction terms proportional to σ^z and σ^x , respectively (see [23]). As we shall see throughout the paper, a longitudinal coupling, in which the bath only induces dephasing in the system without any dissipation, plays a special role. On the other hand, synchronization is found to occur essentially when the transversal coupling (inducing relaxation) overcomes the longitudinal one. To discuss these issues in the simplest possible way, we model the system-environment coupling V_S as

$$V_S = (1+g)(\sigma_1^z + \sigma_2^z) + (1-g)(\sigma_1^x + \sigma_2^x), \quad (3)$$

where we have introduced an anisotropy coefficient $g \in [-1, 1]$.

Notice that, in the limit of $g = 1$, the system Hamiltonian H_S commutes with the total Hamiltonian $H = H_S + H_B + H_{SB}$ and no energy exchange between system and environment can take place, while, for $g \neq 1$, the dynamics of the spin pair always includes some degree of relaxation. The two relevant parameters of the system are the coefficient g and the detuning $\Delta = \omega_2 - \omega_1$. Henceforth, we shall take ω_1 as the scale of energy and inverse time, and therefore, from now on, all of the frequencies are evaluated in units of ω_1 .

Through a rotation, the Hamiltonian model introduced here can be mapped into the more common one describing two Josephson qubits in a noisy environment [24,25]. In fact, H is unitarily equivalent to a set of possible realizations of $H' = H'_S + H'_{SB}$, where the system Hamiltonian and the system-bath interaction Hamiltonian would read, respectively, $H'_S = \Delta_1 \sigma_1^x + \Delta_2 \sigma_2^x + \epsilon_1 \sigma_1^z + \epsilon_2 \sigma_2^z$ and $H'_{SB} = \sqrt{2(1+g^2)}(\sigma_1^z + \sigma_2^z) \sum_k \gamma_k (a_k^\dagger + a_k)$, with the constraint $\Delta_1/\epsilon_1 = \Delta_2/\epsilon_2 = (g+1)/(g-1)$.

The time evolution of the reduced density matrix of the two spins can be calculated using the Bloch-Redfield master equation approach [23]. Up to the second order in the system-bath coupling and in the Markov approximation, we find the following set of equations of motion for the matrix elements of the reduced density matrix in the basis of the eigenstates of H_S :

$$\dot{\rho}_{ab} = -i\omega_{ab}\rho_{ab} - \sum_{mn} R_{abmn}\rho_{mn}, \quad (4)$$

where $\omega_{ab} = E_a - E_b$, and where E_i are the eigenvalues of the unperturbed two-qubit Hamiltonian. The elements of the Redfield tensor are given by

$$R_{abmn} = \delta_{bn} \sum_r S_{ar} S_{rm} \Gamma^+(\omega_{rm}) - S_{am} S_{nb} \Gamma^+(\omega_{am}) + \delta_{am} \sum_r S_{nr} S_{rb} \Gamma^-(\omega_{nr}) - S_{am} S_{nb} \Gamma^-(\omega_{nb}), \quad (5)$$

where $S_{ij} = \langle i|V_S|j\rangle$. Introducing the bath density of states $J(\omega) = \sum_k \gamma_k^2 \delta(\omega - \Omega_k)$, the coefficients Γ^\pm read

$$\Gamma^\pm(x) = \frac{\pi}{8} [J(x) + J(-x)] \left(\coth \frac{\beta x}{2} \mp 1 \right) + \frac{i}{4} \text{P} \int \frac{J(\omega)}{\omega^2 - x^2} \left(x \coth \frac{\beta \omega}{2} \mp \omega \right) d\omega, \quad (6)$$

where P denotes the Cauchy's principal value and where $\beta = 1/k_B T$ is the inverse temperature of the bath. We shall assume an Ohmic environment with a Lorentz-Drude cut-off function, whose spectral density is

$$J(\omega) = \gamma \omega \frac{\omega_c^2}{\omega_c^2 + \omega^2}. \quad (7)$$

The cutoff ω_c is bounded to ensure the validity of the Markovian approximation, $\omega_c \gg \omega_i$, and also for the Bloch-Redfield master equation to give a correct estimation of the renormalizing effects of the bath, $\gamma \omega_c \ll \omega_i$ ($i = 1, 2$).

It is important to remark here that, in general, the Bloch-Redfield second order master equation is known to provide neither a completely positive nor a positive map (see, for instance, [26] for a review). However, usually, if the

system-bath coupling is weak enough, as compared to the energy scales of the system, positivity is not violated. For all the results presented hereafter, we have numerically checked the positivity of the reduced density matrix of the system from the beginning of the evolution (where system and bath are assumed to be uncoupled) until the system reaches or is very close to reaching a final state that can be stationary or oscillating depending on the existence of noise-free channels.

A. Decoherence-free evolution

In the following section, we will show the occurrence of a *significant* time window in which the local observables of the two spins show synchronized oscillations before equilibration takes place. We will require this transient regime to be robust enough (e.g., to last for a very long time), and this will be linked to the appearance of slowly decaying solution of the Bloch-Redfield master equation (4).

In this respect, it is well known that special instances exist in which equilibration does not fully take place because some state of the system happens to be robust against decoherence [27,28], and that this can lead to asymptotic quantum correlations [29]. Indeed, despite the presence of a thermal environment, there are cases where a noiseless evolution can be observed, provided that the full Hamiltonian possesses some special symmetry and that the initial state of the system belongs to a given *decoherence-free* subspace. Such subspaces are found to exist for the cases of (a) identical spins ($\omega_1 = \omega_2$), or (b) purely dephasing dynamics ($g = 1$). In the second case, in particular, the model Hamiltonian becomes exactly solvable and its solution describes the only instance in which the system is not totally dissipative.

Strictly speaking, from the point of view of synchronization, the first of these cases, (a), is trivial (as the precession frequencies are already equal), while the second, (b), is irrelevant (as discussed in Sec. III). However, their analysis will appear to be crucial to understand the emergence of synchronization (and its absence in some regime), and we briefly recall it here.

1. Identical spins

By assuming $\Delta = 0$, irrespective of the value of g , the maximally entangled state $|\psi^-\rangle = (|\uparrow, \downarrow\rangle - |\downarrow, \uparrow\rangle)/\sqrt{2}$ belongs to the kernel of both H_S and V_S [30]. Then, its evolution turns out to be decoherence-free. The special role played by $|\psi^-\rangle$ gives rise to important consequences to the long-time behavior of the system, as for any initial condition not orthogonal to this state the system will never reach a steady state. To make clear the importance of initial conditions chosen in the figures presented hereinafter, we notice that a family of states that does reach a stationary condition at very long times is given by symmetric factorized states, that is, $(\cos \theta|\uparrow\rangle + e^{i\phi} \sin \theta|\downarrow\rangle) \otimes (\cos \theta|\uparrow\rangle + e^{i\phi} \sin \theta|\downarrow\rangle)$, while asymmetric factorized states are in general not orthogonal to $|\psi^-\rangle$.

2. Pure dephasing

For $g = 1$, and independently of the detuning, the bath can only induce dephasing, without any dissipation, since $[H_S, V_S] = 0$ [27,31]. The dynamics of the reduced density

matrix of the system can be calculated exactly using, for instance, the coherent state method introduced in Refs. [27,32]. Labeling with E_i (λ_i) the eigenvalues of $H_S(V_S)$, the density matrix elements, written in the basis of the eigenstates of both H_S and V_S , evolve according to

$$\rho_{ab}(t) = \rho_{ab}(0)e^{-i\omega_{ab}t} \exp\left(-\sum_k \frac{|\gamma_k|^2}{\Omega_k^2} P_{ab,k}\right), \quad (8)$$

with

$$P_{ab,k} = i(\lambda_a^2 - \lambda_b^2) \sin \Omega_k t + 2(\lambda_a - \lambda_b)^2 \sin^2 \frac{\Omega_k t}{2} \coth \frac{\beta \Omega_k}{2}. \quad (9)$$

In the continuum limit we have

$$\rho_{ab}(t) = \rho_{ab}(0)e^{-i\omega_{ab}t} e^{-(\Gamma_{ab} + iL_{ab})t}, \quad (10)$$

where

$$\Gamma_{ab} = 2(\lambda_a - \lambda_b)^2 \int d\omega J(\omega) \omega^{-2} \sin^2 \frac{\omega t}{2} \coth \frac{\beta \omega}{2} \quad (11)$$

and where the Lamb shift is

$$L_{ab} = (\lambda_a^2 - \lambda_b^2) \int d\omega J(\omega) \omega^{-2} \sin \omega t. \quad (12)$$

The bath effect is entirely contained in $\exp[-(\Gamma_{ab} + iL_{ab})t]$. While Γ_{ba} fixes the dephasing rate, L_{ab} introduces a shift in the oscillatory dynamics. In the weak-coupling limit, L is usually negligible and $\Gamma(t)$ is a linear function of time. Notice that the detuning Δ does not play any role in the decoherence process.

The existence of a common basis for H_S and V_S in the pure dephasing limit implies that the four basis states $|1\rangle \equiv |\uparrow\uparrow\rangle$, $|2\rangle \equiv |\uparrow\downarrow\rangle$, $|3\rangle \equiv |\downarrow\uparrow\rangle$, and $|4\rangle \equiv |\downarrow\downarrow\rangle$ would evolve without experiencing any kind of decoherence. Furthermore, since $V_S|\uparrow\downarrow\rangle = V_S|\downarrow\uparrow\rangle = 0$, then, $L_{23} = L_{32} = \Gamma_{23} = \Gamma_{32} = 0$, and the whole subspace spanned by the states $|\uparrow\downarrow\rangle$ and $|\downarrow\uparrow\rangle$ is decoherence-free; that is, only the oscillations due to the free evolution H_S are displayed for such initial states. Among other consequences, a maximally entangled state belonging to this subspace ($|\psi^+\rangle$ or $|\psi^-\rangle$) will remain maximally entangled forever: for instance, by considering $\rho_+(0) = |\psi^+\rangle\langle\psi^+|$, we have

$$\rho_+(t) = \frac{1}{2}(|\uparrow, \downarrow\rangle\langle\uparrow, \downarrow| + |\downarrow, \uparrow\rangle\langle\downarrow, \uparrow| + e^{2i\Delta t}|\downarrow, \uparrow\rangle\langle\uparrow, \downarrow| + e^{-2i\Delta t}|\uparrow, \downarrow\rangle\langle\downarrow, \uparrow|). \quad (13)$$

III. SYNCHRONIZATION

In this section, in analogy with what was done for the case of harmonic oscillator systems in Refs. [12–14], we quantitatively discuss the emergence of synchronization and study the conditions under which the dynamics of two spins with different precession frequencies can exhibit a long-lasting transient regime of phase-locked spin oscillations.

A full characterization of the *local* precessing dynamical behavior of the two spins can be obtained by analyzing the evolution of the average values of their respective Pauli operators. In the absence of noise, the values of $\langle\sigma_1^x(t)\rangle = 2\text{Re}\{\rho_{13}(t) + \rho_{24}(t)\}$ and $\langle\sigma_2^x(t)\rangle = 2\text{Re}\{\rho_{12}(t) + \rho_{34}(t)\}$ would oscillate in time with their respective frequencies $2\omega_1$ and $2\omega_2$ (the

same argument could be applied to $\langle \sigma_1^y \rangle$ and $\langle \sigma_2^y \rangle$ or to any combination in the x - y plane as well. On the other hand, $\langle \sigma_1^z \rangle$ and $\langle \sigma_2^z \rangle$ would be constants of motion. Then, any couple of local spin operators lying in the x - y plane is a good candidate to test whether or not the bath is able to induce synchronous oscillations. For concreteness, in the following we will consider $\langle \sigma_1^x \rangle$ and $\langle \sigma_2^x \rangle$ and study the conditions under which these variables synchronize. Actually, as we shall see, the form of the interaction Hamiltonian adopted in Eq. (3) gives rise to antisynchronization (that is, synchronization in antiphase).

For a quantitative characterization of the degree of synchronization of the time-dependent local spin observables, we will employ a time-correlation coefficient C , which can be defined for any two time-dependent functions $f(t)$ and $f'(t)$ as follows:

$$C_{f,f'}(t, \Delta t) = \frac{\overline{\delta f \delta f'}}{\sqrt{\overline{\delta f^2 \delta f'^2}}}, \quad (14)$$

where the overbar stands for a time average $\overline{f} = \int_t^{t+\Delta t} dt' f(t')/\Delta t$ with time window Δt and $\delta f = f - \overline{f}$ [12]. Phase-locked oscillations lead to $|C| = 1$, while it is easy to see that C decreases to zero for two signals displaying uncorrelated oscillations. We shall take $\langle \sigma_1^x \rangle$ and $\langle \sigma_2^x \rangle$ as local dynamical variables for the two spins, and study the behavior of the synchronization coefficient C as a function of the detuning $\Delta = |\omega_2 - \omega_1|$ and of the anisotropy parameter g .

An example of dynamically induced synchronization is given in Fig. 2. There, we consider the case in which the two spins have similar frequencies ($\omega_2 = 1.02\omega_1$) and are initially prepared in an asymmetric factorized state and show the behavior of $C_{(\sigma_1^x), (\sigma_2^x)}$ (star symbols) for a transversal coupling with the bath ($g = -1$) as a function of time. In the early stage of the evolution (upper inset in Fig. 2), the two functions $\langle \sigma_1^x(t) \rangle$ and $\langle \sigma_2^x(t) \rangle$ oscillate with similar frequencies and with an increasingly different phase. Then, after a transient incoherent time window (middle inset in Fig. 2), finally $C_{(\sigma_1^x), (\sigma_2^x)}$ approaches -1 and the oscillations become antisynchronized (details in the lower inset).

A full characterization of the emergence of synchronization is given in Fig. 3(a) where, by varying both Δ and g , we calculate the time t_{synch} after which $|C|$ reaches the (arbitrarily fixed) threshold value $|C| = 0.92$. As expected from the comparison with the case of detuned harmonic oscillators of Ref. [12], small values of the initial detuning guarantee shorter synchronization times. If the two frequencies are too different, the two spins are not able to synchronize before reaching their steady state. Furthermore, it is clear from this plot that if the environment coupling has a more dephasing nature (that is, for $g > 0$) synchronization does not take place. In particular, for the purely dephasing case discussed above [see Eq. (10)], despite the presence of a decoherence-free subspace, it turns out that only *nonlocal coherences* survive, while *local* spin observables always decay irrespectively of the detuning and of the initial conditions, thus showing that a substantial amount of relaxation is essential for the emergence of synchronization.

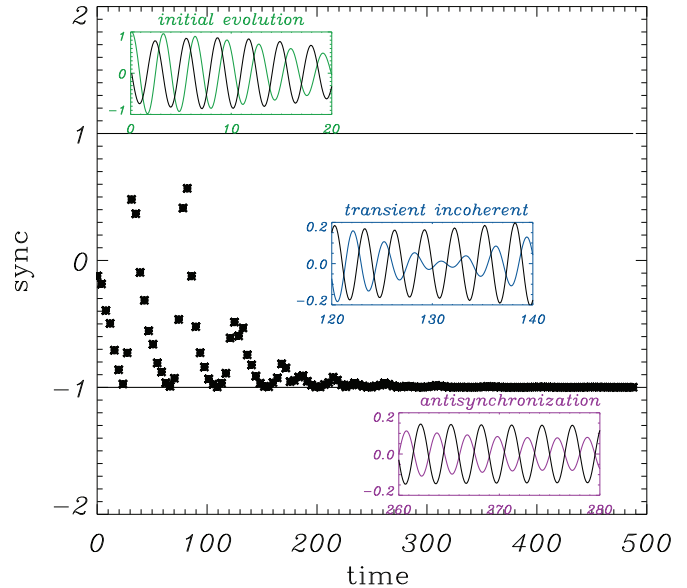


FIG. 2. (Color online) Synchronization coefficient $C_{(\sigma_1^x), (\sigma_2^x)}(t, \Delta t = 6\omega_1)$ (star symbols) as a function of time for $\omega_2 = 1.02\omega_1$ and for $g = -1$. Synchronization is evaluated for partially overlapping time-average windows ($\Delta t = 6\omega_1$), at times $t = 0, 4\omega_1, \dots, 500\omega_1$ [see Eq. (14)]. The bath temperature is $T = \omega_1$, while the cut-off frequency is $\omega_c = 20\omega_1$. Finally, the system-bath coupling strength is $\gamma = 10^{-3}\omega_1$. The initial state is $|\psi(0)\rangle = (\cos \theta_1 |\uparrow\rangle + \sin \theta_1 |\downarrow\rangle) \otimes (\cos \theta_2 |\uparrow\rangle + \sin \theta_2 e^{i\phi_2} |\downarrow\rangle)$ with $\theta_1 = \pi/4$, $\theta_2 = \pi/8$, and $\phi_2 = \pi/2$. Insets show the oscillatory evolution of $\langle \sigma_1^x(t) \rangle$ (lighter line) and $\langle \sigma_2^x(t) \rangle$ (black line) for two different times in the initial transient regime, and after antisynchronization is reached. In all of the plot, time is in units of $1/\omega_1$.

A. Synchronization and dynamical eigenvalues

According to Refs. [12–14], the emergence of synchronization can be explained by considering that, because of dissipation, after a transient time, only the least-damped dynamical eigenmode survives. In order to find a quantitative link between synchronization and the existence of such a transient phase during which only one of the eigenmodes is active, we analyzed the behavior of the eigenvalues of the Redfield tensor, represented as a 16×16 matrix ($R_{abmn} \rightarrow R_{ab, mn}$), as a function of the detuning Δ and of the anisotropy g . Of the 16 eigenvalues, 12 are complex (appearing in complex conjugate pairs), while four are real numbers. These real eigenvalues only influence decays and do not play any role as far as oscillatory dynamics is concerned; then, we shall focus only on the complex ones.

All of the eigenmodes are damped, and the asymptotic dynamics is governed by the least-damped one, with the eigenvalue's real part closest to zero. A significant synchronization window, then, should occur in the case in which the two (pairs of) eigenvalues with largest real parts (smallest in absolute value), say $\lambda_{(1)} = -\lambda_{(1)}^R \pm i\lambda_{(1)}^I$ and $\lambda_{(2)} = -\lambda_{(2)}^R \pm i\lambda_{(2)}^I$, satisfy the relation $\lambda_{(2)}^R \gg \lambda_{(1)}^R$.

In general, however, monitoring the two smallest real parts of the eigenvalues of R is not enough as, in many cases the corresponding eigenmodes do not give a relevant contribution to the expression for the local observables. An

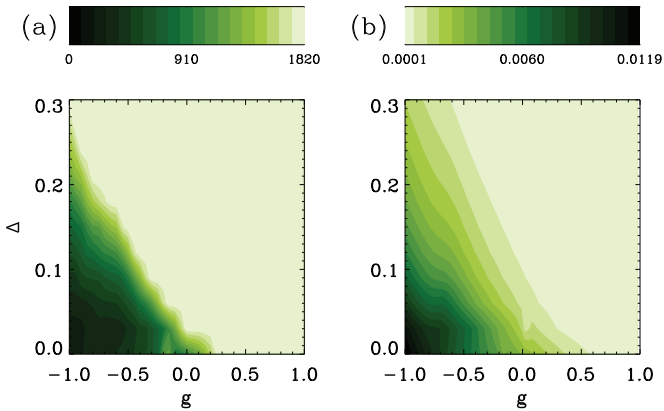


FIG. 3. (Color online) Synchronization maps vs spins detuning Δ (in units of ω_1) and anisotropy coefficient g . (a) Synchronization time t_{synch} , obtained by solution of Eq. (4). This is the time it takes for the synchronization quality factor $C_{(\sigma_1^x(t), \sigma_2^x(t))}$ to reach the threshold value $|C| = 0.92$. Darker colors correspond to synchronous dynamics emerging after a short transient. (b) Difference between the two lowest (real parts of the) eigenvalues of the Redfield tensor R ($\lambda_{(1)}^R, \lambda_{(2)}^R$) with the higher weight in the subspace spanned by σ_1^x and σ_2^x (see text for details). The similarity between the two maps shows that separation between damping rates in the system, appearing for $g < 0$, allows for the emergence of synchronization, which is found to occur for dissipative coupling to the environment and small detunings between the spins. No regime of synchronous oscillation is found if dephasing dominates ($g > 0$), irrespective of the detuning. Bath temperature, cut-off frequency, system-bath coupling, and initial state are the same as in Fig. 2.

explicit and noteworthy example of such a situation occurs for the purely dephasing dynamics that is unable to give rise to synchronization despite the presence of decoherence-free modes.

Then, we considered the two pairs of eigenmodes having more influence on the specific observables we are interested in; and, specifically, among the real parts of the three eigenvalues giving rise to the slowest decays, we selected the two entering $\sigma_1^x(t)$ and $\sigma_2^x(t)$ with the highest weights. The difference between the two decay rates selected in such a way, $\lambda_{(1)}^R - \lambda_{(2)}^R$, is plotted in Fig. 3(b) as a function of g and Δ . By comparing the panels (a) and (b) in Fig. 3, we observe that there is a very good qualitative agreement between t_{synch} and $\lambda_{(1)}^R - \lambda_{(2)}^R$, which confirms our understanding of the emergence of synchronization as a result of the presence of a slowly decaying mode giving a substantial contribution to local spin components.

Since synchronization is due to the robustness of an eigenmode of the Bloch-Redfield tensor, the synchronization frequency ω_{synch} of the two spins is expected to be (very close to) the imaginary part of the corresponding eigenvalue. The agreement between the imaginary part of the eigenvalue corresponding to the mode that decays more slowly and the synchronization frequency is very good also in the presence of relatively strong detuning. Considering, for instance, the case of $\omega_2 = 1.15\omega_1$, assuming $\omega_c = 20\omega_1$, $T = \omega_1$, and $\gamma = 10^{-3}\omega_1$, we have $\text{Im}[\lambda_{(1)}^R] \simeq 2.306\omega_1$, while a numerical estimation performed over 50 antisynchronized cycles gives

$\omega_{\text{synch}}/\omega_1 = 2.306 \pm 0.001$ (where the error comes from time discretization).

B. Discussion

By analyzing the behavior of both t_{synch} and $\lambda_{(1)}^R - \lambda_{(2)}^R$ in Fig. 3, it becomes clear that there is a qualitative difference between a dephasing-dominated and a dissipative interaction with the environment (roughly corresponding to positive and negative values of g). A fully analogous behavior will be found when discussing classical and quantum correlations in Sec. IV. We observe that, when dissipative effects are strong ($g < 0$) the system is able to synchronize in a time t_{synch} that is shorter if Δ is small and longer for large detunings. As a consequence, if Δ is too big (with respect to ω_1), the system reaches its steady state before synchronization can take place.

On the other hand, observing the right parts of Figs. 3(a) and 3(b), we can conclude that if dephasing effects prevail ($g \gtrsim 0$) synchronization does not take place, independently of the detuning. For pure dephasing, in particular, this can be seen directly by looking at the structure of Eq. (10), which implies a common decay factor for both $\langle \sigma_1^x(t) \rangle$ and $\langle \sigma_2^x(t) \rangle$ and the persistence of the two oscillation frequencies ω_1 and ω_2 in the whole transient regime.

One could argue about the dependence of the synchronization diagram of Fig. 3(a) on the initial state. Actually, given the role played by dissipation, the phenomenon is robust against changes in the initial conditions. Synchronous dynamics only arises after the relaxation has washed out any sign of the initial state.

Another possible issue concerns the dependence of synchronization on the bath temperature. While in the case of harmonic oscillators described in Ref. [12] the decay rates of the master equation are temperature independent, this is not true for the spin master equation discussed in this paper. Given the connection between decay rates and synchronization, temperature could be imagined to play a role in determining synchronization times. We analyzed this issue in detail by studying various thermal regimes, but found no qualitative changes with respect to the physical picture given above. In particular, an increase in temperature (with respect to the case $T = \omega_1$ of Fig. 3) would lead to an increase of t_{synch} , but only for large values of the detuning. So, short synchronization times would be almost unaffected, while long synchronization times would become longer by increasing the temperature of the bath.

IV. QUANTUM CORRELATIONS

Having established the regimes in which synchronization takes place in the open dynamics of our spin pair, we now explore a possible connection between the emergence of synchronous oscillations of the two subsystems and the appearance of asymptotic quantum correlations between them. We will measure the correlations using either entanglement or quantum discord (whose definitions are briefly recalled below) to show that their connection with synchronization is guaranteed by dissipation being progressively lost when dephasing overcomes losses.

A. Entanglement and discord

Various indicators have been proposed for the degree of quantumness of the state of a bipartite system. Among them, the entanglement of formation E_F is a well established measure that quantifies the number of singlet states that are necessary to prepare a given entangled state using only local operations and classical communication [33]. For the case of two qubits, it enjoys an analytic expression thanks to its monogamic relationship with the concurrence [34]. The latter can be calculated as $E_C = \max(0, \mu_1 - \mu_2 - \mu_3 - \mu_4)$, where μ_i are the eigenvalues of the Hermitian matrix $R = \sqrt{\sqrt{\rho}\tilde{\rho}\sqrt{\rho}}$ in decreasing order ($\tilde{\rho}$ is the spin flipped matrix of ρ). Finally, $E_F = H[(1 - \sqrt{1 - E_C^2})/2]$, where H is the binary entropy.

Recently, another quantumness quantifier, the quantum discord, has attracted a lot of interest and attention due to its relevance in quantum computing tasks *not* relying on entanglement [35,36]. Given a bipartite state ρ_{ab} , its quantum discord $\delta_{a:b}$ is defined as the difference between two inequivalent quantum versions of the classical mutual information. Quantum mutual information, which is assumed to capture the total amount of correlations between the two parties a and b is defined as $\mathcal{I}(\rho_{ab}) = S(\rho_a) + S(\rho_b) - S(\rho_{ab})$, where ρ_j is the reduced density matrices of subsystem $j = a, b$ and $S(\rho_j) = -\text{Tr}\{\rho_j \log \rho_j\}$ is its von Neumann entropy.

According to Refs. [37,38], \mathcal{I} can be divided into its classical part $\mathcal{C}_{a:b}$ and its quantum part $\delta_{a:b}$. Classical correlations are given by $\mathcal{C}_{a:b}(\rho) = \max_{\{E_j^b\}} [S(\rho_a) - S(a|\{E_j^b\})]$, where the conditional entropy is defined as $S(a|\{E_j^b\}) = \sum_i p_i S(\rho_{a|E_i^b})$, $p_i = \text{Tr}_{ab}(E_i^b \rho)$, and where $\rho_{a|E_i^b} = \text{Tr}_b E_i^b \rho / p_i$ is the density matrix after a positive operator-valued measurement (POVM) $\{E_j^b\}$ has been performed on b . Quantum discord is then defined as the difference between \mathcal{I} and \mathcal{C} : $\delta_{a:b}(\rho) = \min_{\{E_j^b\}} [S(\rho_b) - S(\rho_{ab}) + S(a|\{E_j^b\})]$. Notice that both $\delta_{a:b}$ and $\mathcal{C}_{a:b}$ are asymmetric under the exchange of the two parties, i.e., $\mathcal{C}_{a:b} \neq \mathcal{C}_{b:a}$ and $\delta_{a:b} \neq \delta_{b:a}$.

In order to evaluate $\delta_{a:b}$, a minimization over all possible POVMs has to be performed. In the case of qubits, the optimal projective measurement will have between two and four rank-1 elements [39] (the case of two elements corresponds to orthogonal measurements). Actually, as shown in Ref. [40], orthogonal measurements are sufficient for almost all the states, and where three and four element POVMs outperform them, the numerical difference is always very small and negligible in qualitative analysis. Then, in the following, we shall calculate the discord by limiting the minimization to orthogonal projectors, as usually done in the literature.

B. Long-time behavior of entanglement

Following the discussion in the previous sections, there are two cases in which asymptotic entanglement is expected, provided the initial state is not orthogonal to the singlet state. These are the two cases in which the singlet is found to be a decoherence-free state, namely, (a) for a detuning close to zero, and (b) when dephasing prevails. As shown in Fig. 4, this is indeed the case: For an initial singlet state, an asymptotic entanglement is found both for Δ close to zero and for g close to unity. Out of these specific parameter conditions, the system dynamics displays a rather fast decoherence, leading

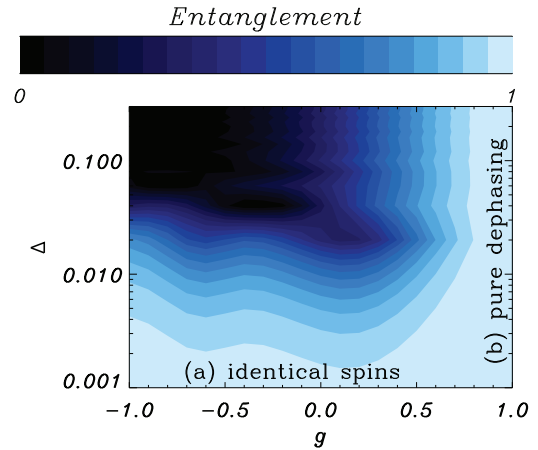


FIG. 4. (Color online) Entanglement of formation at a time $\omega_1 t = 100$ for the case in which the initial state is the singlet, $|\psi^-\rangle$. The robust character of $|\psi^-\rangle$ against decoherence is shown both in the case of identical spins and for pure dephasing, and is a direct manifestation of the occurrence of a decoherence-free dynamics. On the vertical axis, Δ is taken in units of the frequency ω_1 . Fast decoherence would be present with any parameter when starting from most states orthogonal to the singlet, such as a factorized symmetric state. As in the cases discussed before, the bath temperature is $T = \omega_1$, the cut-off frequency is $\omega_c = 20\omega_1$, while $\gamma = 10^{-3}\omega_1$.

to disappearance of entanglement. As a robust entanglement is found to exist under both of these conditions, it is clear that its presence has nothing to do with synchronization. On the other hand, this is not the case for more general quantum correlations.

C. Discord dynamics

Even when entanglement disappears from the system, quantum correlations described by discord can be present and even significantly large. In the following, we explore the temporal dynamics of quantum correlations in different regimes and, in particular, its dynamic generation starting from an initial uncorrelated state. Two completely different scenarios appear in the purely dephasing and dissipative limits, concerning the buildup (and subsequent decay) of both classical correlations and quantum discord, in particular, with respect to the dependence on the detuning between the spins. The two regimes exactly correspond to the emergence (or not) of spontaneous synchronization between the spins.

Indeed, as shown in Fig. 5, two distinct behaviors of quantum discord are found, depending on the relative weight of the transverse and longitudinal components of V_S (inducing relaxation and dephasing, respectively). Starting from a nonsymmetric factorized state, and for negative values of the anisotropy coefficient g , where the fully dissipative term $\sigma_1^x + \sigma_2^x$ dominates, we observe that quantum discord, apart from an abrupt initial increase, shows a monotonous relaxation towards its equilibrium value. The decay of quantum correlations is deeply influenced by the detuning. Indeed, for nearly identical spins (that is, for ω_2/ω_1 close to unity, corresponding to the synchronization region), relaxation is characterized by a long transient regime where quantum discord has a very small decay rate and remains almost frozen.

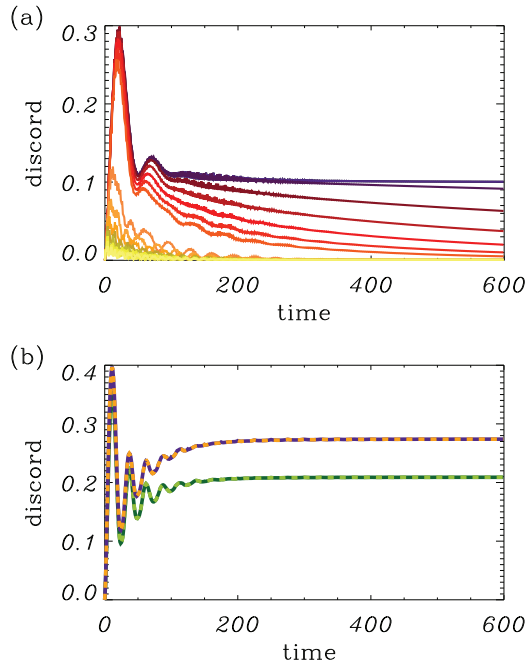


FIG. 5. (Color online) Dynamical generation of quantum discord ($\delta_{a,b}$) starting from a product state for different detunings. (a) Dissipative bath with $g = -1$. Differently colored lines correspond to different detunings Δ from a maximum of $\Delta = 1.25\omega_1$ (lower curve in light color) to $\Delta = 0$ (higher curve in dark color) with intermediate values $\Delta/\omega_1 = \{n \times 0.005\}_{n=1,6}$ for the upper curves and $\Delta/\omega_1 = \{n \times 0.025\}_{n=1,9}$ for the lower ones. The initial state is taken to be $|\psi(0)\rangle = (\cos \theta_1|\uparrow\rangle + \sin \theta_1|\downarrow\rangle) \otimes (\cos \theta_2|\uparrow\rangle + \sin \theta_2|\downarrow\rangle)$ with $\theta_1 = \pi/3, \theta_2 = \pi/3$. (b) Purely dephasing dynamics with $g = 1$. The time evolution of quantum discord is independent of the detuning (different Δ give rise to superimposed curves). The two lines correspond to different initial states, $\theta_1 = \pi/3, \theta_2 = \pi/3$ for the upper curve (which are the same values used in panel (a)), and $\theta_1 = \pi/4, \theta_2 = \pi/8$ for the lower curve. In these plots, time is taken in units of ω_1^{-1} . The bath temperature is $T = \omega_1$, the cut-off frequency is $\omega_c = 20\omega_1$, and $\gamma = 10^{-3}\omega_1$. Time is expressed in units ω_1^{-1} .

The dynamical evolution of $\delta_{a,b}$ for $g = -1$ and for various detunings in Fig. 5(a) shows that the smaller the detuning the higher the “quasistationary” value of the discord maintained during such a long-lasting transient regime.

On the other hand, if the detuning Δ is too large compared with the dissipation rates, the system is not able to build up large enough correlations in the initial evolution and a quick decay of quantum discord is observed. This is illustrated comparing synchronization time with discord after an initial transient in cases where dissipation prevails ($g = -1$ and $g = -0.8$) (Fig. 6). We see that the larger the time taken by the system to synchronize (worse synchronization) the smaller the value maintained by discord. A similar behavior is found for the classical correlations, which, however, are generally smaller than the discord in this system. From this analysis, we conclude that the establishment of transient quantum correlations and the emergence of synchronization are strictly linked in this regime.

A completely different scenario emerges once positive values of g are taken into account. In Fig. 5(b) we consider the other extreme case of pure dephasing ($g = 1$). In this case,

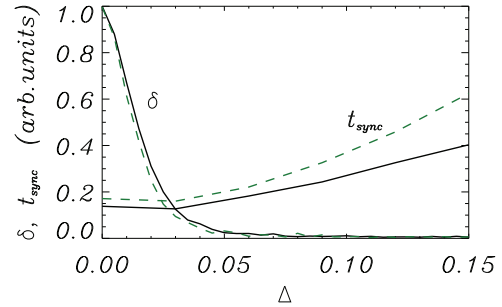


FIG. 6. (Color online) Value of quantum discord [$\delta_{a,b}(t = 300)$] and synchronization time t_{synch} starting from a symmetric product state for $g = -1$ (continuous lines) and $g = -0.8$ (dashed lines) when increasing the detuning Δ (expressed in ω_1 units). For the sake of comparison, discord and synchronization time are rescaled. As before, the bath temperature is $T = \omega_1$, the cut-off frequency is $\omega_c = 20\omega_1$, and $\gamma = 10^{-3}\omega_1$.

the discord transient dynamics does not depend on Δ , while its asymptotic value changes for different initial conditions. As we can see from Fig. 5(b), the dephasing channel is able to generate an asymptotically robust amount of quantum discord starting from a product state (the same is true for classical correlations). On the other hand, it would be impossible for this channel to build up entanglement.

The asymptotic value of discord can be calculated by considering that the channel maps the initial state $\rho(0)$ onto

$$\rho^\infty = \begin{pmatrix} \rho_{11}(0) & 0 & 0 & 0 \\ 0 & \rho_{22}(0) & \rho_{23}(0)e^{-i\xi} & 0 \\ 0 & \rho_{32}(0)e^{i\xi} & \rho_{33}(0) & 0 \\ 0 & 0 & 0 & \rho_{44}(0) \end{pmatrix}, \quad (15)$$

where $\xi = 2\Delta t$, and with the density matrix written in the computational basis $\{|\uparrow\uparrow\rangle, |\uparrow\downarrow\rangle, |\downarrow\uparrow\rangle, |\downarrow\downarrow\rangle\}$. An analytic expression for discord and classical correlations of this class of states can be obtained by using the results of Chen *et al.* in Ref. [41], who showed that the conditional entropy is minimized either by using the eigenstates of σ_x or the ones of σ_z to perform the measurement on party b . In our case, the optimal measurement to be performed in order to obtain the minimum conditional entropy is given by the projections along the eigenstates of σ_x . The maximum achievable discord, for an initially factorized state, is obtained if $\rho_{ij}(0) = 1/4$ for any of the nonempty entries of ρ^∞ . Its value is $\delta_{\text{max}} \simeq 0.312$ and the corresponding classical correlations are $\mathcal{C}_{\text{max}} \simeq 0.188$.

As follows from our previous considerations, in the case of identical spins the system will not completely thermalize for any value of g , due to the presence of the decoherence-free singlet state, unless it is initially prepared in a state orthogonal to $|\psi^-\rangle$. With the exception of this special case with $\Delta = 0$, and of the purely dephasing case $g = 1$, the system always reaches a thermal equilibrium state in a time that becomes shorter and shorter as the detuning increases. For small detunings, however, the transient regime displays a large time window where robust quantum correlations are found, in spite of dissipation.

The long-time behavior of quantum discord and of classical correlations for any value of g is illustrated in Fig. 7. Both δ and

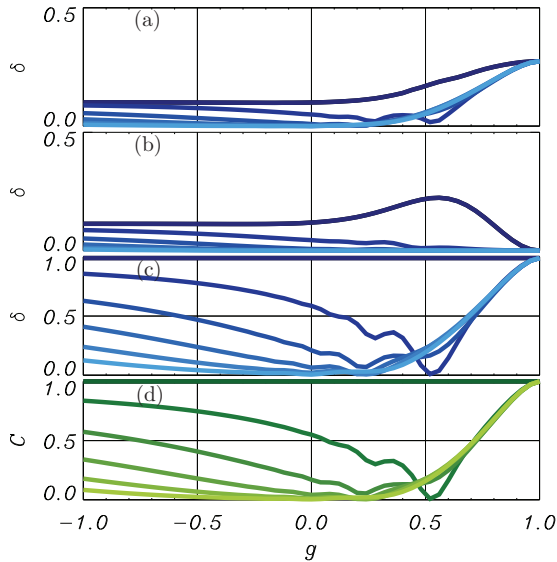


FIG. 7. (Color online) Long-time behavior of discord δ and of classical correlations \mathcal{C} , evaluated at $t = 800/\omega_1$ as a function of the anisotropy parameter g . In all of the panels, the six different curves correspond to detunings increasing from $\Delta = 0$ (higher curves) up to $\Delta = 0.025\omega_1$ (lower curves). The different panels correspond to different initial conditions: In (a) we have chosen a product state with $\theta_1 = \pi/4, \theta_2 = \pi/8$; in (b) the maximally entangled state $|\phi^+\rangle$, while panels (c) and (d) are obtained by taking $|\psi^-\rangle$ as the initial state of the spin pair. The bath temperature and the cut-off frequency are the same as in any other plot ($T = \omega_1$ and $\omega_c = 20\omega_1$), while $\gamma = 10^{-3}\omega_1$.

\mathcal{C} are calculated, for the fixed time $\omega_1 t = 800$, as a function of g and for a set of values of the detuning Δ . The separation between the “dissipative regime” and the “dephasing regime” is clear from this plot. In the “dephasing regime” there is a coalescence of all the lines and the detuning does not play any special role, consistent with what is shown in Fig. 5(b). In contrast, the qualitative behavior described for $g = -1$ in Fig. 5(a) persists up to around $g = 0$. In other words, both the discord and the classical correlations \mathcal{C} display an increasing robustness against dissipation as Δ decreases. This behavior (with the dependence on Δ when dissipation prevails and the robustness of correlations for small detunings) is definitely analogous to what we have found for the time-correlation coefficient describing synchronization.

V. CONCLUSIONS

We have investigated the long-time dynamics of two spins interacting through a common thermal bath and have shown that, depending on the relative weights of the environment-induced dissipation and dephasing, two qualitatively different dynamic regimes are observed for both spin-spin correlations and mutual synchronization.

The presence of dissipation induces a time scale separation in the decay rates of the eigenmodes of the Redfield tensor, which govern the system’s evolution. This allows one to observe spontaneous synchronization between the local observables of the two spins. When the precessions of the two spins are synchronous, long-time classical and quantum correlations (as measured by quantum discord) are found for the spin pair, which become more and more robust against decoherence as the synchronization time gets shorter (which is the case for small detunings).

On the other hand, a channel in which dephasing prevails is not able to generate any time scale separation and cannot support any kind of dynamical synchronization. Long-time (and even asymptotic) quantum correlations between the spins may exist in this case, but they have a completely different origin. Indeed, they are due to the existence of a decoherence-free subspace which prevents the decay of part of the initial coherences of the total system, while allowing for the dynamic cancellation of some others, in a way that enables the possibility of generating quantum correlations even from an initially factorized state. Remarkably, this mechanism does not allow for the generation of entanglement, but only of quantum discord [42]. When the dissipative nature of the coupling with the environment prevails, instead, quantum discord is generated precisely because of the emergence of synchronization.

ACKNOWLEDGMENTS

This work was funded by MICINN, MINECO, and FEDER under Grants No. FIS2007-60327 (FISICOS) and No. FIS2011-23526 (TIQS), and by Balearic Islands Government. G.L.G. acknowledges financial support by Compagnia di San Paolo, by Science Foundation of Ireland under Project No. 10/IN.1/I2979, and by EU commission (IP AQUITE and STREP PICC). The visiting professors program of the University of Balearic Islands and COST Action MP1209 are also acknowledged.

-
- [1] A. Pikovsky, M. Rosenblum, and J. Kurths, *Synchronization: A Universal Concept in Nonlinear Sciences* (Cambridge University Press, Cambridge, 2001).
 - [2] S. H. Strogatz, *Nonlinear Dynamics And Chaos: With Applications To Physics, Biology, Chemistry, and Engineering* (Westview Press, Boulder, CO, 2001).
 - [3] Ch. Huygens (Hugenii), *Horologium Oscillatorium* (Apud F. Muguet, Paris, France (1673). English translation: *The Pendulum Clock* (Iowa State University Press, Ames, 1986).
 - [4] A. Arenas, A. Díaz-Guilera, J. Kurths, Y. Moreno, and C. Zhou, *Phys. Rep.* **469**, 93 (2008).
 - [5] K. Wiesenfeld, P. Colet, and S. H. Strogatz, *Phys. Rev. Lett.* **76**, 404 (1996).
 - [6] S. Kaka *et al.*, *Nature (London)* **437**, 389 (2005).
 - [7] S.-B. Shim, M. Imboden, and P. Mohanty, *Science* **316**, 95 (2007).
 - [8] G. Heinrich, M. Ludwig, J. Qian, B. Kubala, and F. Marquardt, *Phys. Rev. Lett.* **107**, 043603 (2011).
 - [9] C. A. Holmes, C. P. Meaney, and G. J. Milburn, *Phys. Rev. E* **85**, 066203 (2012).
 - [10] M. Zhang, G. S. Wiederhecker, S. Manipatruni, A. Barnard, P. McEuen, and M. Lipson, *Phys. Rev. Lett.* **109**, 233906 (2012).

- [11] A. Mari, A. Farace, N. Didier, V. Giovannetti, and R. Fazio, *Phys. Rev. Lett.* **111**, 103605 (2013).
- [12] G. L. Giorgi, F. Galve, G. Manzano, P. Colet, and R. Zambrini, *Phys. Rev. A* **85**, 052101 (2012).
- [13] G. Manzano, F. Galve, and R. Zambrini, *Phys. Rev. A* **87**, 032114 (2013).
- [14] G. Manzano, F. Galve, E. Hernandez-Gracia, G. L. Giorgi, and R. Zambrini, *Sci. Rep.* **3**, 1439 (2013).
- [15] I. Goychuk, J. Casado-Pascual, M. Morillo, J. Lehmann, and P. Hänggi, *Phys. Rev. Lett.* **97**, 210601 (2006).
- [16] O. V. Zhirov and D. L. Shepelyansky, *Phys. Rev. Lett.* **100**, 014101 (2008); O. Astafiev, K. Inomata, A. O. Niskanen, T. Yamamoto, Yu. A. Pashkin, Y. Nakamura, and J. S. Tsai, *Nature (London)* **449**, 588 (2007).
- [17] O. V. Zhirov and D. L. Shepelyansky, *Phys. Rev. B* **80**, 014519 (2009).
- [18] F. Galve, L. A. Pachon, and D. Zueco, *Phys. Rev. Lett.* **105**, 180501 (2010); V. Vedral, *Phys. Rev. Focus* **26**, 17 (2010).
- [19] F. Francica, S. Maniscalco, J. Piilo, F. Plastina, and K.-A. Suominen, *Phys. Rev. A* **79**, 032310 (2009).
- [20] F. Benatti, R. Floreanini, and U. Marzolino, *Europhys. Lett.* **88**, 20011 (2009); *Phys. Rev. A* **81**, 012105 (2010); F. F. Fanchini, L. K. Castelano, and A. O. Caldeira, *New J. Phys.* **12**, 073009 (2010).
- [21] Y. Liu, F. Piechon, and J. N. Fuchs, *Europhys. Lett.* **103**, 17007 (2013).
- [22] P. P. Orth, D. Roosen, W. Hofstetter, and K. Le Hur, *Phys. Rev. B* **82**, 144423 (2010).
- [23] A. J. Leggett *et al.*, *Rev. Mod. Phys.* **59**, 1 (1987); U. Weiss, *Quantum Dissipative Systems* (World Scientific, Singapore, 1999).
- [24] Y. Makhlin, G. Schön, and A. Shnirman, *Rev. Mod. Phys.* **73**, 357 (2001).
- [25] M. J. Storcz, F. Hellmann, C. Hrelescu, and F. K. Wilhelm, *Phys. Rev. A* **72**, 052314 (2005).
- [26] F. Benatti and R. Floreanini, *Int. J. Mod. Phys. B* **19**, 3063 (2005).
- [27] G. M. Palma, K.-A. Suominen, and A. K. Ekert, *Proc. R. Soc. London, Ser. A* **452**, 567 (1996).
- [28] P. Zanardi and M. Rasetti, *Phys. Rev. Lett.* **79**, 3306 (1997); D. A. Lidar, I. L. Chuang, and K. B. Whaley, *ibid.* **81**, 2594 (1998); L. M. Duan and G. C. Guo, *Phys. Rev. A* **58**, 3491 (1998).
- [29] S. Maniscalco, F. Francica, R. L. Zaffino, N. Lo Gullo, and F. Plastina, *Phys. Rev. Lett.* **100**, 090503 (2008).
- [30] The fact that the state $|\psi^-\rangle$ is free from decoherence depends on the relative sign (or, in general, relative phase) between σ_1^x and σ_2^x in the coupling term in Eq. (3). It is immediately seen that, by applying symmetry considerations, it would be $|\psi^+\rangle$ not to decohere for a coupling of the form $\sigma_1^x - \sigma_2^x$.
- [31] J. H. Reina, L. Quiroga, and N. F. Johnson, *Phys. Rev. A* **65**, 032326 (2002); D. V. Averin and R. Fazio, *JETP Lett.* **78**, 664 (2003).
- [32] D. Mozyrsky and V. Privman, *J. Stat. Phys.* **91**, 787 (1998).
- [33] R. Horodecki, P. Horodecki, M. Horodecki, and K. Horodecki, *Rev. Mod. Phys.* **81**, 865 (2009).
- [34] W. K. Wootters, *Phys. Rev. Lett.* **80**, 2245 (1998).
- [35] E. Knill and R. Laflamme, *Phys. Rev. Lett.* **81**, 5672 (1998); A. Datta, A. Shaji, and C. M. Caves, *ibid.* **100**, 050502 (2008); B. P. Lanyon, M. Barbieri, M. P. Almeida, and A. G. White, *ibid.* **101**, 200501 (2008).
- [36] K. Modi, A. Brodutch, H. Cable, T. Paterek, and V. Vedral, *Rev. Mod. Phys.* **84**, 1655 (2012).
- [37] H. Ollivier and W. H. Zurek, *Phys. Rev. Lett.* **88**, 017901 (2001).
- [38] L. Henderson and V. Vedral, *J. Phys. A* **34**, 6899 (2001).
- [39] G. M. D'Ariano, P. L. Lopresti, and P. Perinotti, *J. Phys. A: Math. Gen.* **38**, 5979 (2005).
- [40] F. Galve, G. L. Giorgi, and R. Zambrini, *Europhys. Lett.* **96**, 40005 (2011).
- [41] Q. Chen, C. Zhang, S. Yu, X. X. Yi, and C. H. Oh, *Phys. Rev. A* **84**, 042313 (2011).
- [42] The generation of quantum discord has been discussed at length in T. Abad, V. Karimipour, and L. Memarzadeh, *Phys. Rev. A* **86**, 062316 (2012); F. Galve, F. Plastina, M. G. A. Paris, and R. Zambrini, *Phys. Rev. Lett.* **110**, 010501 (2013); X. Hu, H. Fan, D. L. Zhou, and W.-M. Liu, *Phys. Rev. A* **87**, 032340 (2013).